doi:10.1007/s11589-012-0866-y

Scale lengths of heterogeneities under Tibet*

Yingcai Zheng†

Department of Earth, Atmospheric and Planetary Sciences, Massachusetts Institute of Technology, MA 02139, *USA*

Abstract Important information about small-scale heterogeneities is hardly accessible by the traditional deterministic seismic tomography. Fluctuations of the phase and the logarithmic amplitude of direct teleseismic plane P waves can be used to characterize small-scale heterogeneities. Seismic data recorded by the Hi-CLIMB array are used to analyze the average power spectrum of the small-scale velocity heterogeneities under Tibet. Coherence functions of the logarithmic amplitude and the phase fluctuations due to different earthquakes from different back azimuths show consistent characteristics, indicating that fluctuations are due to heterogeneities under the stations. Assuming that the heterogeneities are statistically stationary and distributed within a layer, we invert for the average heterogeneity spectrum by fitting both the logarithmic amplitude and the phase coherence data. Multiscale nature of the heterogeneity is evident. The inverted power spectrum is "red" at the large-scale end, meaning that the power spectrum decreases as the length scale decreases. Such a decreasing trend stops at smaller scales ∼20–50 km and 10 km. This may indicate that mantle convection is not effective in destroying smaller heterogeneities.

Key words: **seismic tomography; mantle heterogeneity; scattering; coherence function**

CLC number: P315.3 **Document code**: A

1 Introduction

Mapping seismic velocity variations in the interior of the Earth provides a powerful way to interrogate dynamics of the Earth (Dziewonski, 2005). Subducted slabs are cold and usually associated with fast seismic velocities; and hot upwellings like the deep mantle plumes and partial melts under the mid ocean ridges are commonly associated with slow velocities. These features can be traced deep into the mantle by seismic tomography (Grand et al., 1997). The spatial resolution of global tomography is on the order of thousands of kilometers. However many geological units such as the oceanic crust thickness, seamounts, and slabs are on the order of tens of kilometers. In the deterministic tomography, gross volumetric averages of such structures largely miss the geological complexity, giving very reductionist visions of the structure and processes occurring in the dynamic mantle system. Although progresses have been made in terms of new inversion methods and more seismometers deployed, we are still far from producing tomograms with a spatial resolution on the scale of these interesting tectonic units. In the traveltime tomography, there is significant power in the traveltime residuals that are not accounted for by the final velocity model (Maceira et al., 2011). The residuals can be explained by random heterogeneities in the model, which are missed by the deterministic tomography.

Therefore, it is natural to view the seismic velocity variations in terms of a deterministic component plus a stochastic component. Small-scale statistical velocity variations also carry important information about the Earth's dynamics. The perturbation strengths and length scales of these small-scale heterogeneities provide a way to study convective mixing of the mantle, which may have far-reaching consequences in petrology, mineralogy and geochemistry (Bercovici, 2007).

The first statistical study of the Earth interior dated back to Aki (1973), which predated the modern deterministic seismic tomography. Following Aki's initial work to characterize heterogeneities under the Large Aperture Seismic Array (LASA), Montana, several other studies were carried out for Norwegian Seismic Array (NORSAR) and southern India (Capon, 1974; Capon and Berteussen, 1974; Berteussen et al.,

* **Received** 8 October 2012; **accepted in revised form** 12 November 2012; **published** 10 December 2012.

† **Corresponding author. e-mail**: yczheng@mit.edu

1977; Flatté and Wu, 1988). For inverting the heterogeneity spectrum, several types of coherence functions are proposed. Aki (1973) used the transverse coherence function (TCF) or the Chernov theory (Chernov, 1960). Flatté and Wu (1988) extended the method to the angular coherence function (ACF). And then Wu and Flatté (1990) and Chen and Aki (1991) independently proposed the joint transverse and angular coherence function (JTACF). However, these important theoretical progresses are all for a homogeneous background velocity. Recent work by Zheng and Wu (2008) has extended the theories to having a 1D variable background velocity, suitable for global studies.

Establishing statistical characteristics of random heterogeneities under various global localities and different tectonic units is useful to understand mantle convection and mixing. In this paper, we document results under Tibet using the Hi-CLIMB (Himalayan–Tibetan Continental Lithosphere during Mountain Building) data (Nábelěk et al., 2009).

2 Data and method

In this paper, we perform the transverse coherence function (TCF) analysis; the assumption is that the incident wave is a plane wave. We used seismic data from the Hi-CLIMB seismic experiment (Figure 1). The Hi-CLIMB seismic line extends from the interior of the Tibet southwards to Nepal. The southernmost stations are in the Ganga sedimentary basin where thick (≥6 km) sediments are documented. For those stations, unusual amplifications of seismic waves are observed due to soft sediments. Therefore, in our analysis, we exclude data from those stations and only use stations whose elevation is greater than 4 300 m. We only use direct P waves from distant earthquakes whose depths are greater than 40 km and epicentral distances greater than 40 degrees to avoid upper mantle triplications. The earthquakes are mainly in subduction zones around the west Pacific and Indonesia (Figure 1). We loosely divide the earthquakes into three groups. The nominal Japan group includes events in Alaska, Kuriles, Japan and Marianas, whose backazimuths are less than 100 degrees. The Tonga group consists of earthquakes with back azimuths larger than 100 degrees and epicentral distances greater than 60 degrees. The Indonesia group has earthquakes with backazimuths larger than 100 degrees and epicentral distances greater than 40 but less than 60 degrees. The TCF measures the spatial correlation of the natural logarithmic amplitude ($\log A$) or phase between two stations at a particular frequency. For each event, we measure the $\log A$ (or phase) at 0.5 Hz and remove the linear trend to obtain the $\log A$ (or phase) fluctuations across the seismic array. These fluctuations are then used to form the coherence functions that depend on the distance between the stations. Coherence functions from multiple earthquakes are then averaged and resampled using the bootstrap technique (Efron and Tibshirani, 1993) to compute the statistical errors and to test for statistical significance. It is remarkable that TCFs for both $\log A$ and phase for the three separate event groups are similar (Figure 2), which strongly argues that the origin of heterogeneities giving rise to these fluctuations is below the Hi-CLIMB seismic stations. Using these $\log A$ and phase TCF data, we can invert for the heterogeneity spectrum under stations.

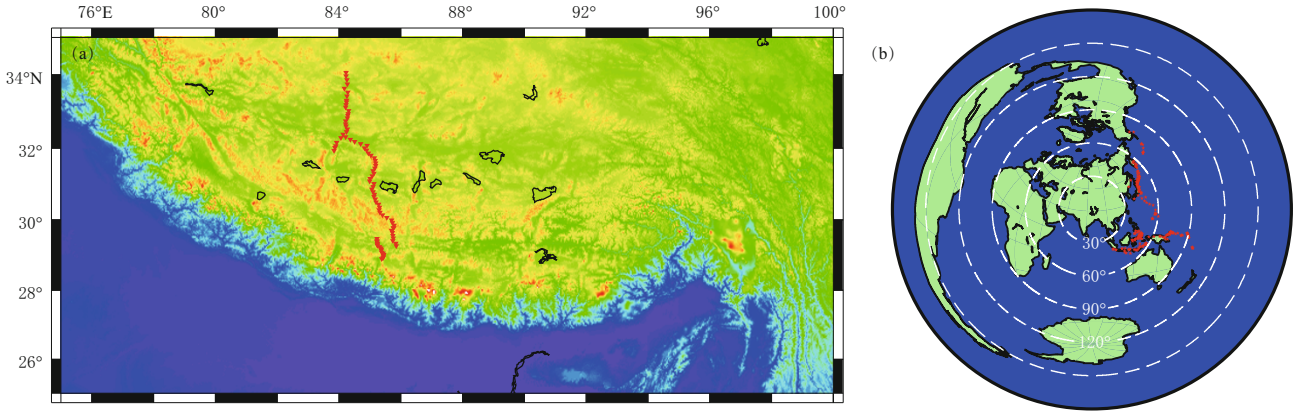

Figure 1 (a) A map showing Hi-CLIMB seismic stations with elevation greater than 4 300 m; (b) Earthquakes (red stars) used in this study. White dashed circles are epicentral distances (every 30°) from a nominal point (longitude 84.9°E, latitude 31.5°N) in Tibet.

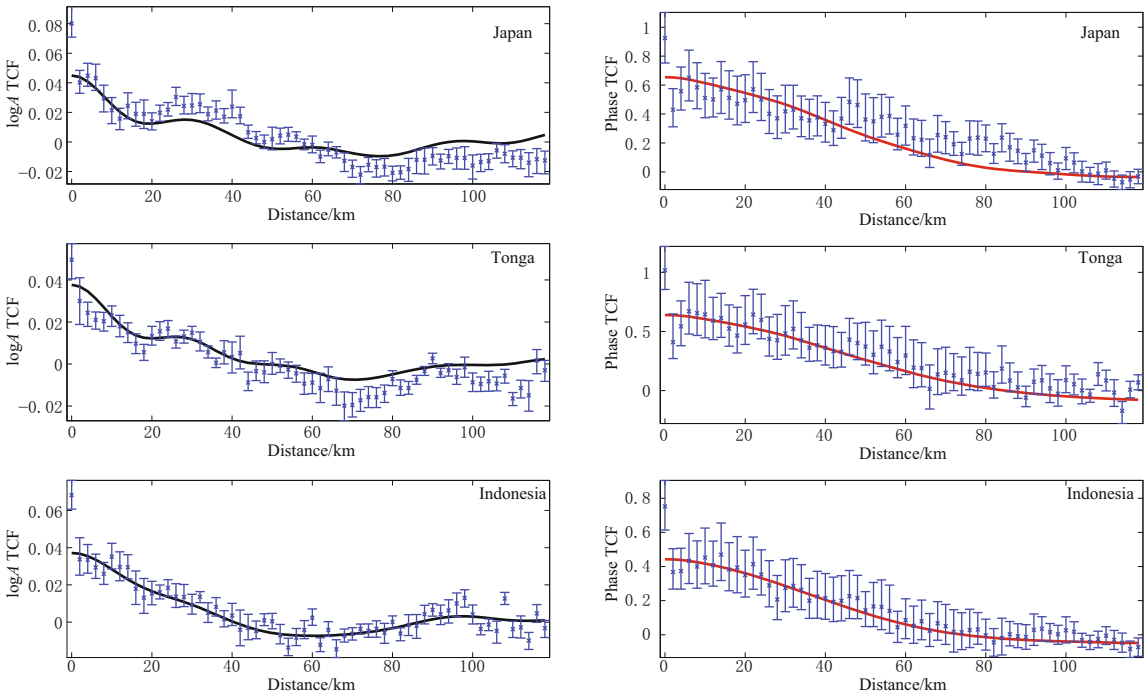

Figure 2 Comparison between observed TCF data (dots with error bars of 90% confidence) and modeled TCFs (thick lines) using heterogeneity spectra in Figure 3 for Japan, Tonga and Indonesia earthquakes.

The unknown depth-dependent heterogeneity spectrum $P(z,\kappa)$ (where z is the depth variable and κ is the horizontal wavenumber) and the observed coherence functions can be related mathematically (Zheng and Wu, 2008). In the frequency (ω) domain, log$A$ (u) and phase (ϕ) coherence functions between two plane waves identified by their incidence angles, $\boldsymbol{\phi}_1$ and $\boldsymbol{\phi}_2$ (in 3D geometry, $\boldsymbol{\phi}$ includes both the back azimuth and the incident angle and it points in the same direction as the slowness vector; but in the TCF case, $\boldsymbol{\phi}_1$=$\boldsymbol{\phi}_2$), can be written as, respectively

$$\langle u(\boldsymbol{x}_1)u(\boldsymbol{x}_2)\rangle \approx (2\pi)^{-1}\int_0^L \mathrm{d}z a^2(z)\cdot \int_0^\infty \mathrm{J}_0[\kappa R(z)]\sin^2[\omega\vartheta(z)]P(z,\kappa)\kappa\mathrm{d}\kappa \quad (1)$$

and

$$\langle \phi(\boldsymbol{x}_1)\phi(\boldsymbol{x}_2)\rangle \approx (2\pi)^{-1}\int_0^L \mathrm{d}z a^2(z)\cdot \int_0^\infty \mathrm{J}_0[\kappa R(z)]\cos^2[\omega\vartheta(z)]P(z,\kappa)\kappa\mathrm{d}\kappa \quad (2)$$

where $u(\boldsymbol{x})$ is the measurement of the log$A$ fluctuation at station $\boldsymbol{x}$ for the plane wave. Therefore, $\langle u(\boldsymbol{x}_1)u(\boldsymbol{x}_2)\rangle$ is the observed log$A$ coherence function which depends on the spatial lag $\boldsymbol{\rho}$=$\boldsymbol{x}_2$−$\boldsymbol{x}_1$ between station $\boldsymbol{x}_2$ and $\boldsymbol{x}_1$. However, in the TCF case and if the random medium is statistically isotropic (e.g., independent of direction), the coherence function only depends on the station distance ρ=$|\boldsymbol{\rho}|$=$R(z)$. The symbol $\langle\cdot\rangle$ is the ensemble average operator over random media and $\mathrm{J}_0(\cdot)$ the Bessel function. L is the thickness of the heterogeneous region. The WKBJ amplitude term reads

$$a(z) = \frac{k(z)^2}{\eta(z)}, \quad (3)$$

where $k(z)=\omega/c(z)$ is the background wavenumber at depth z and $\eta(z)$ is the vertical wavenumber. The phase function ϑ is defined as

$$\vartheta(z) = \frac{1}{2}\frac{\kappa^2}{\omega^2}\frac{\mathrm{d}^2\tau(p)}{\mathrm{d}p^2}, \quad (4)$$

where

$$\tau(z) = \int_0^z \sqrt{c^{-2}(z)-p^2}\mathrm{d}z \quad (5)$$

is the familiar τ function (e.g., Buland and Chapman, 1983) which contains the kinematic information for the wave propagation; $c(z)$ is the background velocity at depth z and p is the slowness of the plane wave. The validity of equations (1) and (2) has been verified by full-wave finite difference numerical simulation for wave propagation in random media in Zheng and Wu (2008).

In equation (1) (or (2)), the left hand side is the observed coherence function using log$A$ (or phase) fluctuation data and the right hand side is a weighted summation of the spatially-filtered depth-dependent heterogeneity spectra $P(z,\kappa)$ over the depth z.

The inverse problem consists of solving for the spectrum $P(z,\kappa)$ given the observed coherence functions. We use a vector $\boldsymbol{m}$ to denote the unknown spectrum $P(\kappa_i)\geq 0$ and A for the matrix of kernels. In computing A, one has to pay attention to the oscillatory integral. Assuming the heterogeneous medium is just one stationary layer, we can use the standard least squares method to minimize

$$||A\boldsymbol{m}-\boldsymbol{d}||_2,$$

in which $\boldsymbol{d}$ contains the observables (i.e., log$A$ and phase coherence functions on the Earth's surface). One can also control the smoothness of the model $\boldsymbol{m}$ by minimizing the following objective function with positivity constraint for $\boldsymbol{m}$ (Constable et al., 1987):

$$||A\boldsymbol{m}-\boldsymbol{d}||_2+\mu||\partial^2\boldsymbol{m}||_2,$$

in which

$$\partial^2=\begin{bmatrix} 0 & 0 & 0 & & \\ 1 & -2 & 1 & & \\ & \ddots & \ddots & \ddots & \\ & & 1 & -2 & 1 \\ & & & 0 & 0 \end{bmatrix}$$

is the smoothing regularization operator. This is equivalent to solving the following problem in the least squares sense:

$$\begin{bmatrix} A \\ \sqrt{\mu}\partial \end{bmatrix}\boldsymbol{m}=\begin{bmatrix} \boldsymbol{d} \\ \boldsymbol{0} \end{bmatrix}.$$

For a multi-layered random model, the similar inverse procedure follows.

3 Inversion results

For each event group (Japan, Tonga and Indonesia), we simultaneously use both the log$A$ and the phase TCFs for that group to invert for the heterogeneity spectrum under the stations. We assume that heterogeneities exist in a single layer and are statistically stationary in space. In the inversion, this unknown heterogeneous layer is superimposed on a background velocity model, which is the IASPEI91 model (Kennett and Engdahl, 1991). The TCF inversion has weak constraint on the layer thickness (Wu and Xie, 1991). So we can only invert for the average statistical property of heterogeneities for the layer. Because the phase TCF has large sensitivity at the shallow depths and the log$A$ TCF is sensitive to deeper structures, the layer thickness cannot be arbitrary. If the layer thickness is too small, only the phase TCF can be fitted well but not the log$A$. On the other hand, if the layer thickness is too large, log$A$ data can be fitted but not the phase. Earlier studies assumed that the heterogeneities were in the lithosphere. So we can adopt a layer thickness of 120 km. The layer thickness has a trade-off with the random heterogeneity perturbation strength. Using different layer thicknesses can only affect the root-mean-square (RMS) velocity of the heterogeneities, not the shape of the inverted spectrum. Therefore, the scale lengths of the heterogeneities can still be inferred. In our parameterization of the spectrum, the largest length scale is 400 km and the smallest is 20 km. This is consistent with the array aperture and the average station spacing. Within this range, we invert for 61 discrete spectral values. Linear interpolation between discrete spectra is adopted in the inversion. We tried different regularization parameter μ and the optimal value is determined by the well-known L-curve, which corresponds to a smooth model that can fit the data (Figure 2). We also inspected other μ values around the optimal value. The results are stable with respect to the choice of μ. The inverted models show that the spectral amplitude decreases from the largest scale to about 80 km (Figure 3). This part of the spectrum explains the long-wavelength features for both the log$A$ and phase TCFs. However, in order to fit the short-wavelength rapid fluctuations in the log$A$ TCF, small-scale heterogeneities must be used. Heterogeneities on the scales of ~50 km and ~25 km are also inverted (Figure 3). We have to clarify here that the heterogeneity scale is meant to be the spatial wavelength of the heterogeneities. Over the spatial distance of a wavelength, there are a positive anomaly and a negative anomaly. Random realizations show that these inverted spectra (Figure 3), if isotropic, correspond to RMS velocity fluctuations of ~1.9%, 1.8% and 1.6%, for the Japan, Tonga and Indonesia groups, respectively, with respect to the background velocity model.

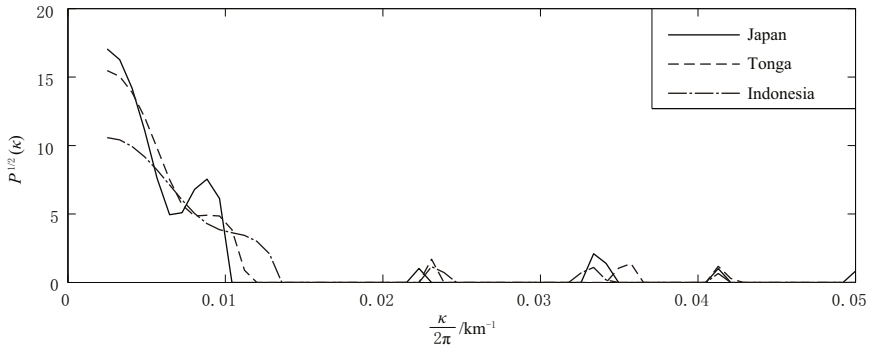

Figure 3 Inverted heterogeneity spectra at 0.5 Hz. For each event group, we simultaneously model both the phase and the log$A$ TCF data.

4 Discussion and conclusions

Regarding inversion of small-scale statistical heterogeneities, early studies assumed that the heterogeneities are Gaussian in statistics (e.g., Aki, 1973) or power-law (Bataille and Flatté, 1988; Flatté and Wu, 1988; Sato and Fehler, 1998) by a parametric approach. However, we directly invert for the average heterogeneity spectrum using both log$A$ and phase data without assuming a specific form for the spectrum *a priori*. Our results showed that the average heterogeneity spectrum under the Tibet is not a single-scale Gaussian type spectrum but includes several length scales. This is a robust observation despite that the heterogeneity layer thickness is only approximately constrained. It is also plausible that under Tibet several layers of random heterogeneities exist, with each having a distinct spectrum. However, given the depth resolving power of the TCF, inverting multi-layer spectra has not been possible. However with JTACF data this is feasible (Zheng and Wu, 2008).

Global deterministic seismology revealed significant velocity variations in the mantle on the length scale of thousands of km, which are frequently interpreted as cold downwellings and hot upwellings in term of plates and plumes. Due to limitation in the methodology and data coverage, such deterministic methods cannot produce information about small-scale heterogeneities. However information about length scales on the order of tens of km is very useful because they correspond to spatial dimensions of familiar and pervasive tectonic units such as subducted oceanic plates, subducted oceanic crusts, depleted harzburgite layers at the mid ocean ridges, etc. This represents a gap in scale. Our method in principle can provide such information even for the deep lower mantle. Small-scale heterogeneity spectra may yield information how the mantle is convecting. For large-scale heterogeneities (>500 km), global and regional tomography showed that the spectrum is power-law and essentially red (Chevrot et al., 1998), meaning the mantle convection primarily destroy large scale heterogeneities. However, in our results, we observe that the spectral amplitude decreases at the large-scale end. But the same decaying behavior stops at length scales of tens of km (Figure 3). This may indicate that the mantle convection is not efficient in destroying small-scale heterogeneities.

Acknowledgements I thank Dr. Shiyong Zhou and two other anonymous reviewers for comments and useful suggestions. I also thank Junmeng Zhao for discussions and invitation for this contribution. The Earth Resources Laboratory at MIT provides facilities for me to conduct this research that is an extension to an earlier effort supported by an NSF Grant No. EAR-0838359.

References

Aki K (1973). Scattering of P waves under the Montana Lasa. *J Geophys Res* **78**(8): 1 334–1 346.

Bataille K D and Flatté S M (1988). Inhomogeneities near the core-mantle boundary inferred from short-period scattered PKP waves recorded at the Global Digital Seismograph Network. *J Geophys Res* **93**(B12): 15 057–15 064.

Bercovici D (2007). Mantle dynamics past, present, and future: An introduction and overview. In: Gerald S ed. *Treatise on Geophysics*. Elsevier, Amsterdam, 1–30.

Berteussen K A, Husebye E S, Mereu R F and Ram A (1977). Quantitative assessment of the crust-upper mantle heterogeneities beneath the Gauribidanur seismic array in southern India. *Earth Planet Sci Lett* **37**(2): 326–332.

Buland R and Chapman C H (1983). The computation of seismic travel times. *Bull Seismol Soc Am* **73**(5): 1 271–

1 302.

Capon J (1974). Characterization of crust and upper mantle structure under LASA as a random medium. *Bull Seismol Soc Am* **64**(1): 235–266.

Capon J and Berteussen K A (1974). A random medium analysis of crust and upper mantle structure under NORSAR. *Geophys Res Lett* **1**(7): 327–328.

Chen X and Aki K (1991). General coherence functions for amplitude and phase fluctuations in a randomly heterogeneous medium. *Geophys J Int* **105**(1): 155–162.

Chernov L A (1960). *Wave Propagation in a Random Medium*. McGraw-Hill, New York, 168pp.

Chevrot S, Montagner J P and Snieder R (1998). The spectrum of tomographic earth models. *Geophys J Int* **133**(3): 783–788.

Constable S C, Parker R L and Constable C G (1987). Occam's inversion: A practical algorithm for generating smooth models from electromagnetic sounding data. *Geophysics* **52**(3): 289–300.

Dziewonski A M (2005). The robust aspects of global seismic tomography. *Geological Society of America Special Papers* **388**: 147–154.

Efron B and Tibshirani R J (1993). *An Introduction to the Bootstrap*. Chapman & Hall/CRC, New York, 456pp.

Flatté S M and Wu R S (1988). Small-scale structure in the lithosphere and asthenosphere deduced from arrival time and amplitude fluctuations at NORSAR. *J Geophys Res* **93**(B6): 6 601–6 614.

Grand S P, van der Hilst R D and Widiyantoro S (1997). Global seismic tomography: a snapshot of convection in the Earth. *GSA Today* **7**(4): 1–7.

Kennett B L N and Engdahl E R (1991). Traveltimes for global earthquake location and phase identification. *Geophys J Int* **105**(2): 429–465.

Maceira M, Larmat C, Rowe C A, Allen R M and Obrebski M J (2011). Validating seismic imaging methods and 3D seismic velocity models. *Eos Trans AGU* **92**: S41A-2182.

Nábělek J, Hetényi G, Vergne J, Sapkota S, Kafle B, Jiang M, Su H, Chen J, Huang B S and the Hi-CILMB Team (2009). Underplating in the Himalaya-Tibet collision zone revealed by the Hi-CLIMB experiment. *Science* **325**(5946): 1 371–1 374.

Sato H and Fehler M (1998). *Seismic Wave Propagation and Scattering in the Heterogeneous Earth*. Springer-Verlag, New York, 308pp.

Wu R S and Flatté S M (1990). Transmission fluctuations across an array and heterogeneities in the crust and upper mantle. *Pure Appl Geophys* **132**(1-2): 175–196.

Wu R S and Xie X B (1991). Numerical tests of stochastic tomography. *Phys Earth Planet Inter* **67**: 180–193.

Zheng Y and Wu R S (2008). Theory of transmission fluctuations in a depth-dependent background medium. In: Sato H and Fehler M eds. *Earth Heterogeneity and Scattering Effects on Seismic Waves*. Academic Press, Amsterdam, 21–41.